





Generalized normal mode expansion method for open and lossy periodic structures

SRAVYA RAO,^{1,*}  GUILLAUME LE SAUX,² YONATAN SIVAN,¹  AND PARRY Y. CHEN¹

¹School of Electrical and Computer Engineering, Ben-Gurion University of the Negev, Beersheba, Israel

²Department of Materials Engineering, Ilse Katz Institute for Nanoscale Science and Technology, Ben-Gurion University of the Negev, Beersheba, Israel

*Corresponding author: sravya@post.bgu.ac.il

Received 6 January 2022; revised 2 March 2022; accepted 17 March 2022; posted 17 March 2022; published 19 April 2022

We describe and demonstrate the extension of permittivity mode expansion, which is also known as generalized normal mode expansion (GENOME), to open and lossy periodic structures. The resulting expansion gives a complete spatial characterization of any open periodic structure, via the quasi-periodic Green's tensor, by a complete, discrete set of modes rather than a continuum. The method has been validated by comparing our expansion of an open waveguide array with a direct scattering calculation. Good agreement was obtained regardless of the source location or detuning from resonance. © 2022 Optica Publishing Group

<https://doi.org/10.1364/JOSAB.452555>

1. INTRODUCTION

Periodic nanophotonic structures such as photonic crystal fibers [1,2], photonic crystal waveguides [3–5] and hole arrays [6] enable the generation, control and manipulation of the propagation of light [7–9], making them attractive for various electro-optic applications like the inhibition of spontaneous emission for thresholdless lasing [10], slow light propagation [3,11], enhancing nonlinear effects [12,13], and optical switching [14,15]. Optimal design of such nanophotonic structures requires characterization of the complete spatial distribution of local electric fields. In particular, many quantum-optical applications require knowledge of the field distribution and the associated photonic density of states (DOS) [16] in the presence of (single) quantum emitters, which can be obtained directly from Green's tensor \vec{G} .

Unfortunately, the characterization of Green's tensor for any nontrivial geometry requires repeated simulation for every different source position and orientation. An efficient way to treat all these cases simultaneously is to use modal expansion methods since these provide the Green's tensor everywhere in space from a single simulation. In modal expansions, we represent the electromagnetic fields and the Green's tensor as a weighted sum of eigenfunctions of the nanophotonic structure; in many cases, this also has the computational advantage of requiring the use of only a few eigenmodes, a description which may also provide useful physical insights. Modal expansion formalisms are well investigated for lossless and closed periodic structures using eigenfrequency modes. These eigenfrequency modes are stationary states and have real frequencies; it is a manifestation of the closed Hermitian system, which also means these modes form a complete, discrete, and orthogonal basis set.

However, when the structure involves absorbing materials or allows radiation leakage to the far field (i.e., open structures in which the modes couple to free space), the eigenvalue must be complex to represent the lack of energy conservation. Complex eigenfrequency modes are also known as quasi-normal modes (QNMs) [17] or resonant states [18]. Unfortunately, the use of QNMs for open structures creates new problems due to their exponentially diverging far-field behavior, which requires nontrivial normalization schemes and the inclusion of the continuum of background modes to reproduce the physically correct solution in the background medium [17–20]. The details of the calculation and implementation of the QNMs/resonant states, together with a discussion of the various solutions to their limitations (e.g., due to the complexity of numerical implementation or incompleteness of the QNM expansion [21]) are described in [19,22].

QNMs have been successfully employed for various periodic structures [19,23–26]. Many of those used plane wave expansion to calculate the quasi-normal Bloch modes (QNBMs), where the open sides of the structure were treated with different boundary conditions [19,20]; others found the modes via the poles of the scattering matrix [25] and via perturbation methods [27]. The latter studies required additional discretization schemes for the continuum of background modes; the standard numerical approach is to use the perfectly matched layer (PML) as the boundary condition in the open directions. However, the resulting nonphysical PML modes require a complicated sorting procedure [19,28]. Furthermore, if the periodic structure has dispersive materials, the associated eigenvalue equation becomes nonlinear. Algorithms for nonlinear eigenvalue problems tend to require more human intervention and are less reliable.

In addition, the eigenmodes of dispersive media are linearly dependent [17,29], thus requiring a more elaborate basis expansion procedure [17,30]. An alternative way to treat material dispersion is to use auxiliary fields [31], which linearizes the eigenvalue problem for materials whose permittivity is well-described by a sum of Lorentzian responses. However, this necessitates solving a larger number of differential equations.

One way to circumvent all the difficulties associated with complex frequency modes is by using eigenpermittivity modes as the basis for modal expansion [21,32,33]. In this approach, the radiative nature of the open structure is compensated by gain via the imaginary part of the eigenpermittivity, yielding modes that are stationary states without field divergences in the background. Furthermore, the eigenpermittivity modes always satisfy the bi-orthogonality property, making them a complete and discrete orthogonal basis set. Even for dispersive materials, these eigenmodes are still generated by a linear eigenvalue equation, thus keeping the computation of Green’s tensor simple and straightforward.

Previous studies of eigenpermittivity modes have treated isolated open resonators [32,34–39]. Modal expansion for Green’s tensor via eigenpermittivity modes, known as the generalized normal mode expansion (GENOME), was demonstrated in [21] along with a numerical solver for permittivity modes implemented using commercially available software. The formalism of permittivity modes was further extended to clusters of open resonators through hybridization [32,33,40,41] and its implementation for nontrivially shaped nanoparticle clusters was described in [42]. Hybridization was also used to generate the modes of periodic arrays of particles; this approach was proceeded by computing lattice sums over an infinite array [32]. Unfortunately, such approaches can be applied only to isolated scatterers, and not to waveguide-like structures such as in Fig. 1. A different approach applicable to any periodic array was proposed in [43]; it focused on determining the effective index of an array of spherical resonators by solving the equations for the Fourier components originating from the integral form of the eigenvalue equation in the electrostatic limit.

In this paper, we propose a more general formalism to compute the electrodynamic Green’s tensor of any open and lossy periodic structure using eigenpermittivity modes (i.e., avoiding

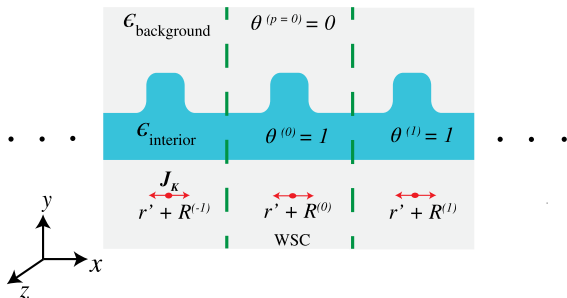


Fig. 1. Example of an open periodic ridge waveguide structure in 2D space, which is periodic along the x direction and is open along the y direction. The structure is excited by a periodic array of phased point dipole sources in each unit cell whose positions are indicated by $\mathbf{r}' + \mathbf{R}^{(p)}$. The unit cell of the waveguide is defined by the step function $\theta^{(p)}(\mathbf{r}')$, which is unity inside the interior of the p^{th} index unit cell and zero elsewhere. The $p = 0$ unit cell is known as the Weigner–Seitz cell (WSC) [44].

the electrostatic approximation). This formalism provides a robust and accurate solution, which is exact up to truncation.

The paper has three additional sections. In Section 2, we develop the GENOME formalism for open and lossy periodic structures, obtaining the quasi-periodic Green’s tensor. In Section 3, we demonstrate its numerical implementation for a periodic waveguide array [45] along with a comprehensive comparison of GENOME against a direct excitation solution based on COMSOL Multiphysics. Section 4 summarizes the work and discusses potential next steps.

2. FORMULATION

In this section, we adapt the derivation of the GNOME of [21] to periodic systems. We begin with the vector Helmholtz equation,

$$\nabla \times (\nabla \times \mathbf{E}(\mathbf{r})) - k^2 \epsilon(\mathbf{r}) \mathbf{E} = i\omega\mu_0 \mathbf{J}(\mathbf{r}), \quad (1)$$

where we assumed a harmonic $e^{-i\omega t}$ time variation and non-magnetic media. Here, \mathbf{E} is the electric field vector, $k = \omega/c$ is the vacuum wavenumber (ω being the photon frequency and c being the speed of light in vacuum), \mathbf{J} represents an externally imposed source, and $\epsilon(\mathbf{r})$ is the permittivity profile. For simplicity, we assume that the structure consists of only two constituent materials: an interior with permittivity ϵ_i and a background with ϵ_b . However, it is relatively easy to generalize the formulation to account, for example, for a substrate and a superstrate (host) of different permittivities [16]. The assumption permits the manipulation of Eq. (1) to yield

$$\nabla \times (\nabla \times \mathbf{E}) - k^2 \epsilon_b \mathbf{E} = i\omega\mu_0 \mathbf{J} + k^2 (\epsilon(\mathbf{r}) - \epsilon_b) \mathbf{E}. \quad (2)$$

Since the operator on the left-hand side (LHS) of Eq. (2) is no longer a function of \mathbf{r} , Eq. (2) can, in principle, be solved by superposing the “source” terms on the right-hand side with the appropriate Green’s tensor of uniform space $\bar{\bar{G}}_0$ [46], which results in the Lippmann–Schwinger equation,

$$\mathbf{E}(\mathbf{r}) = \mathbf{E}_0(\mathbf{r}) + k^2 \int \bar{\bar{G}}_0(\mathbf{r} - \mathbf{r}'; \omega) (\epsilon(\mathbf{r}') - \epsilon_b) \mathbf{E}(\mathbf{r}') d\mathbf{r}', \quad (3)$$

where $\mathbf{E}_0(\mathbf{r})$ represents the known field of the external sources in a uniform background; namely,

$$\mathbf{E}_0(\mathbf{r}) = i\omega\mu_0 \int \bar{\bar{G}}_0(\mathbf{r} - \mathbf{r}'; \omega) \mathbf{J}(\mathbf{r}') d\mathbf{r}'. \quad (4)$$

Then, one could, in principle, follow the GENOME procedure to solve the Lippmann–Schwinger equation as in [21]. However, we now depart from previous derivations to incorporate Floquet–Bloch periodic conditions.

Specifically, we now consider an open periodic structure, with periodicity in at least one dimension and open boundary conditions in at least another. Optionally, the structure can also have continuous translational symmetry along a third dimension. The example shown in Fig. 1 has all three types of the above boundary conditions. As an aside, the formalism below can also be applied to structures with only periodic and translationally invariant conditions.

The periodicity in the structure is represented by the permittivity profile as $\epsilon(\mathbf{r}) = \epsilon(\mathbf{r} + \mathbf{R}^{(p)})$, where

$$\mathbf{R}^{(p)} = \sum_{i=1}^{d_\Lambda} n_i \mathbf{a}_i, \quad (5)$$

is a translational lattice vector and \mathbf{a}_i are the primitive lattice vectors, d_Λ is the number of periodic dimensions and p indexes the unit cells, represented by a single integer (n_1) for $d_\Lambda = 1$ and a pair of integers (n_1, n_2) for $d_\Lambda = 2$. We can represent the external source $\mathbf{J}(\mathbf{r})$ as a coherent superposition of sources in each unit cell. This enables us to treat the coherent excitation of all unit cells, such as plane wave illumination, or a coherent excitation of near-field sources, as in a nonlinear wave mixing problem. This coherent excitation relates the sources in each unit cell via Floquet–Bloch (FB) periodicity; i.e.,

$$J_{\mathbf{K}}(\mathbf{r} + \mathbf{R}^{(p)}) = J_{\mathbf{K}}(\mathbf{r})e^{i\mathbf{K} \cdot \mathbf{R}^{(p)}}, \quad (6)$$

where \mathbf{K} represents the phase delay between adjacent unit cells, also commonly known as the Bloch vector. This FB periodicity allows the simulation domain to be reduced to a single unit cell. The fields also obey FB conditions,

$$E_{\mathbf{K}}(\mathbf{r} + \mathbf{R}^{(p)}) = E_{\mathbf{K}}(\mathbf{r})e^{i\mathbf{K} \cdot \mathbf{R}^{(p)}}. \quad (7)$$

Then, we can define the quasi-periodic Green's tensor of uniform space as the solution of

$$\begin{aligned} \nabla \times (\nabla \times \bar{\bar{G}}_{0,\mathbf{K}}) - k^2 \epsilon_b \bar{\bar{G}}_{0,\mathbf{K}} \\ = \bar{\bar{I}} \sum_{p=-\infty}^{\infty} \delta^3(\mathbf{r} - \mathbf{r}' - \mathbf{R}^{(p)}) e^{i\mathbf{K} \cdot \mathbf{R}^{(p)}}, \end{aligned} \quad (8)$$

where $\bar{\bar{I}}$ is the identity tensor. Here, $\bar{\bar{G}}_{0,\mathbf{K}}$ obeys the same boundary conditions obeyed by $E_{\mathbf{K}}$,

$$\bar{\bar{G}}_{0,\mathbf{K}}(\mathbf{r} + \mathbf{R}^{(p)}, \mathbf{r}'; \omega) = \bar{\bar{G}}_{0,\mathbf{K}}(\mathbf{r}, \mathbf{r}'; \omega) e^{i\mathbf{K} \cdot \mathbf{R}^{(p)}}, \quad (9)$$

Or, in terms of the source position,

$$\bar{\bar{G}}_{0,\mathbf{K}}(\mathbf{r}, \mathbf{r}' + \mathbf{R}^{(p)}; \omega) = \bar{\bar{G}}_{0,\mathbf{K}}(\mathbf{r}, \mathbf{r}'; \omega) e^{-i\mathbf{K} \cdot \mathbf{R}^{(p)}}. \quad (10)$$

Using the quasi-periodic Green's tensor, we can write the solution of Eq. (3) for a periodic structure as a Lippmann–Schwinger equation:

$$\begin{aligned} E_{\mathbf{K}}(\mathbf{r}) = E_{0,\mathbf{K}}(\mathbf{r}) + k^2(\epsilon_i - \epsilon_b) \\ \times \int_{\text{WSC}} \bar{\bar{G}}_{0,\mathbf{K}}(\mathbf{r}, \mathbf{r}'; \omega) \theta^{(p=0)}(\mathbf{r}') E_{\mathbf{K}}(\mathbf{r}') d\mathbf{r}', \end{aligned} \quad (11)$$

where

$$\epsilon(\mathbf{r}') - \epsilon_b = (\epsilon_i - \epsilon_b) \theta^{(p)}(\mathbf{r}'),$$

and $\theta^{(p)}(\mathbf{r}')$ is a step function that is unity inside the interior of the p^{th} unit cell and zero elsewhere. For convenience, we have chosen to consider the $p = 0$ unit cell. Here, the field $E_{0,\mathbf{K}}(\mathbf{r})$

produced by external sources in a uniform background is also computed from the central unit cell. It is given by

$$E_{0,\mathbf{K}}(\mathbf{r}) = i\omega\mu_0 \int_{\text{WSC}} \bar{\bar{G}}_{0,\mathbf{K}}(\mathbf{r}, \mathbf{r}'; \omega) J_{\mathbf{K}}(\mathbf{r}') d\mathbf{r}', \quad (12)$$

where WSC represents integration over the Weigner–Seitz unit cell. The next step is to define the eigenpermittivity modes and determine the modal expansion solution of the Lippmann–Schwinger equation [Eq. (11)]. We define the eigenvalue equation for the eigenpermittivity modes $\epsilon_{\mathbf{K},m}$ of the periodic structure in Appendix A, and derive the modal expansion solution,

$$\begin{aligned} E_{\mathbf{K}} = E_{0,\mathbf{K}} + \frac{i}{\omega\epsilon_0} \sum_m E_{\mathbf{K},m} \frac{\epsilon_i - \epsilon_b}{(\epsilon_{\mathbf{K},m} - \epsilon_i)(\epsilon_{\mathbf{K},m} - \epsilon_b)} \\ \times \int_{\text{WSC}} E_{\mathbf{K},m}^\dagger \cdot J_{\mathbf{K}} d\mathbf{r}, \end{aligned} \quad (13)$$

which expresses the total field $E_{\mathbf{K}}$, as a combination of $E_{0,\mathbf{K}}$ from Eq. (12) and a sum over the eigenmodes of the structure. The contribution of each eigenmode is weighted by the “detuning” of the corresponding eigenvalue $\epsilon_{\mathbf{K},m}$ from the actual permittivity, ϵ_i , and by the overlap integral $\int_{\text{WSC}} E_{\mathbf{K},m}^\dagger \cdot J_{\mathbf{K}} d\mathbf{r}$, which represents the interaction between the source and each eigenmode. The explicit form of the adjoint field $E_{\mathbf{K}}^\dagger(\mathbf{r})$ is discussed in Appendix B. Next, we obtain the desired normal mode expansion of the quasi-periodic Green's tensor:

$$\begin{aligned} \bar{\bar{G}}_{\mathbf{K}}(\mathbf{r}, \mathbf{r}'; \omega) = \bar{\bar{G}}_{0,\mathbf{K}}(\mathbf{r}, \mathbf{r}'; \omega) + \frac{1}{k^2} \sum_m \frac{\epsilon_i - \epsilon_b}{(\epsilon_{\mathbf{K},m} - \epsilon_i)(\epsilon_{\mathbf{K},m} - \epsilon_b)} \\ \times E_{\mathbf{K},m}(\mathbf{r}) \otimes E_{\mathbf{K},m}^\dagger(\mathbf{r}'), \end{aligned} \quad (14)$$

where $\bar{\bar{G}}_{0,\mathbf{K}}(\mathbf{r}, \mathbf{r}'; \omega)$ is the quasi-periodic Green's tensor of the uniform background [Eq. (8)].

The expansion solution will be valid everywhere in space, even though the eigenmodes form a complete set only in the interior of the inclusion. This follows from the property of the Lippmann–Schwinger equation; i.e., representation of the total field in terms of the field inside the inclusion geometry.

3. NUMERICAL EXAMPLE

In this section, we demonstrate the GENOME formalism derived on the example of a periodic ridge waveguide in 2D space. Its unit cell is shown in Fig. 2. This structure is periodic in the x direction, is open in the y direction, and has continuous-translational invariance in the z direction. In this 2D geometry, the point-dipole source is of infinitesimal extent in-plane ($x - y$), but is infinite in the z direction.

The first step is to compute the eigenpermittivity modes by the COMSOL Multiphysics eigensolver using the substitution trick described in [21]. In this simulation, we apply the FB periodicity (with Bloch wavenumber K) in the x direction. The simulation domain in the y direction is enclosed by perfectly matched layers to avoid unwanted reflections. Once these eigenmodes are found, they are normalized according to Eq. (A9) in Appendix A within the inclusion interior.

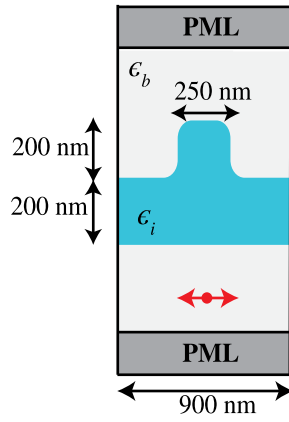


Fig. 2. Simulated geometry, a ridge waveguide with periodicity along the horizontal direction, and the lattice constant $L = 900$ nm. The edges of the ridge are rounded with a radius of curvature of 70 nm. The open sides of the structure (i.e., in the y direction) are enclosed by perfectly matched layers (PML). The structure is excited by an in-plane, point-dipole source (that extends into the out-of-plane dimension), whose position is indicated by the dot on the double-headed arrow, and whose orientation is parallel to the arrow.

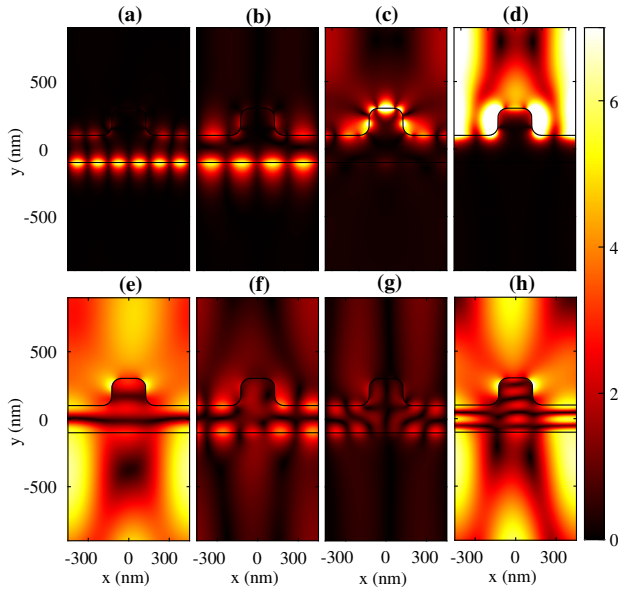


Fig. 3. Electric field profiles of different sets of eigenpermittivity modes for $KL = 0.09$, $\lambda = 700$ nm, and $\beta = 0$ rad/m. All plots show $|\mathbf{E}_x|$, superimposed with the outline of the waveguide geometry. The first row shows plasmonic modes with eigenpermittivities of (a) $\epsilon_m = -1.23 - 0.0003i$, (b) $\epsilon_m = -1.65 - 0.0086i$, (c) $\epsilon_m = -1.21 - 0.1188i$, and (d) $\epsilon_m = -6.26 - 2.2535i$. The second row shows dielectric modes with eigenpermittivity values of (e) $\epsilon_m = 3.752 - 2.0686i$, (f) $\epsilon_m = 3.752 - 2.0686i$, (g) $\epsilon_m = 7.512 - 0.1070i$, and (h) $\epsilon_m = 12.8914 - 2.2608i$.

In Fig. 3, we present the field profile of a few eigenpermittivity modes for $KL = 0.09$ and the out-of-plane (z direction) propagation constant of $\beta = 0$ rad/m. Following [32,34,38], we categorize these modes as either plasmonic or dielectric, depending on the sign of the real part of eigenpermittivity. The first row displays the plasmonic modes (with eigenpermittivities of $\text{Re}[\epsilon_m] < 0$) and the second row displays dielectric modes (with

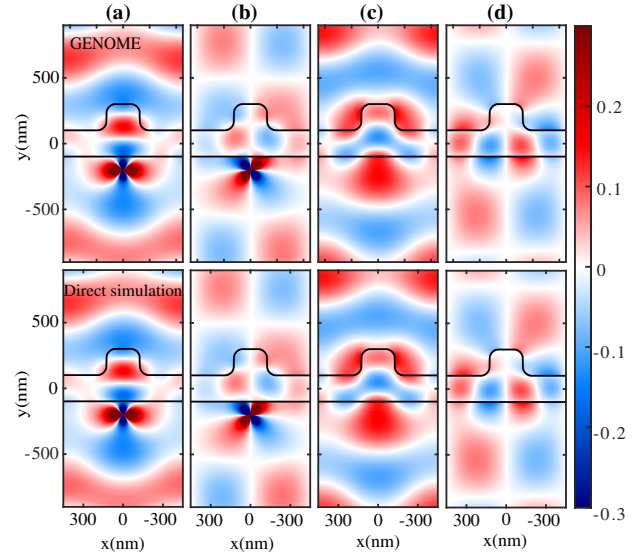


Fig. 4. Validation of GENOME against a direct scattering simulation for a waveguide of permittivity $\epsilon_i = 4.7$, with background permittivity $\epsilon_b = 1$, excited by an x polarized dipole source placed as shown in Fig. 2 with $\lambda = 700$ nm and $KL = 0.09$. The first row shows the results of GENOME computed from Eq. (14) and the second row shows the results of direct simulation using COMSOL. Each column shows a different component of Green's tensor corresponding to (a) $\text{Re}(G_{xx})$, (b) $\text{Re}(G_{yx})$, (c) $\text{Im}(G_{xx})$, and (d) $\text{Im}(G_{yx})$. We have superimposed an outline of the inclusion geometry.

$\text{Re}[\epsilon_m] > 0$). Figures 3(d), 3(e), and 3(h) show bright modes; namely, a relatively high amplitude in the background medium compared to the others; this radiative feature is associated with a large value of $\text{Im}[\epsilon_m]$.

Next, we compute the GENOME solution (14) by projecting the eigenpermittivity modes onto the source, and adding the free-space quasi-periodic Green's tensor, $\bar{G}_{0,K}(\mathbf{r}, \mathbf{r}', \omega)$, for which a rapidly converging solution is derived in Appendix C. To validate the GENOME solution, we compare it to a direct scattering simulation produced by COMSOL MULTIPHYSICS for a given source position, polarization, and Bloch vector. Figure 4 compares the field profiles for the inclusion permittivity $\epsilon_i = 4.7$, $KL = 0.09$, and out-of plane propagation constant, $\beta = 0$ rad/m. We see that GENOME obtains a qualitative agreement with the direct COMSOL simulation for both the real and imaginary parts of the Green's tensor. A similar comparison is shown in Fig. 5 for a different value of inclusion permittivity, $\epsilon_i = -6 + 2i$, but with the same excitation conditions.

To obtain a quantitative measure of the agreement, we compute the spatially resolved relative difference between the two approaches, which is shown in Fig. 6. We use

$$\Delta \text{Re}(G_{xx}) = 10 \log_{10} \left| \text{Re} \left(\frac{G_{xx} - G_{xx, \text{COMSOL}}}{\max(G_{xx, \text{COMSOL}})} \right) \right|, \quad (15)$$

which is defined, for example, on the real part of the Green's tensor component G_{xx} . The first row corresponds to the dielectric inclusion geometry ($\epsilon_i = 4.7$), where the relative difference shows that GENOME has achieved good accuracy. However, the agreement of the real parts of Green's tensor is worse near

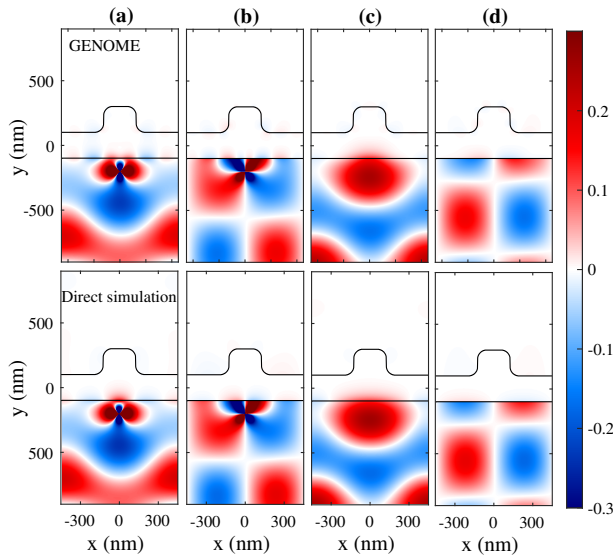


Fig. 5. Same as in Fig. 4, but for waveguide permittivity $\epsilon_i = -6 + 2i$. The first row shows the results of GENOME while the second row shows the results of direct simulation using COMSOL. Each column shows a different component of Green's tensor corresponding to (a) $\text{Re}(G_{xx})$, (b) $\text{Re}(G_{yx})$, (c) $\text{Im}(G_{xx})$, and (d) $\text{Im}(G_{yx})$.

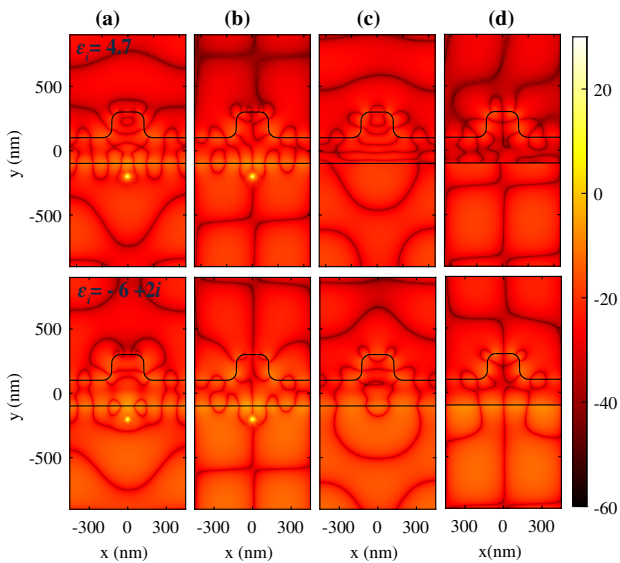


Fig. 6. Relative difference between GENOME and COMSOL direct simulation on a dB scale. The first row corresponds to $\epsilon_i = 4.7$ while the second row corresponds to $\epsilon_i = -6 + 2i$ with columns showing the relative difference in (a) $\text{Re}(G_{xx})$, (b) $\text{Re}(G_{yx})$, (c) $\text{Im}(G_{xx})$, and (d) $\text{Im}(G_{yx})$.

the source; the error originates from the inability of the direct COMSOL simulation to reproduce the diverging field at the source origin. Additionally, there is limited agreement at the inclusion boundary, which happens because of the difficulty to sufficiently find many plasmonic modes using the eigensolver because of the strong field confinement at the metal–dielectric interface. This inaccuracy is more pronounced for the plasmonic inclusion case, as shown in the second row of Fig. 6.

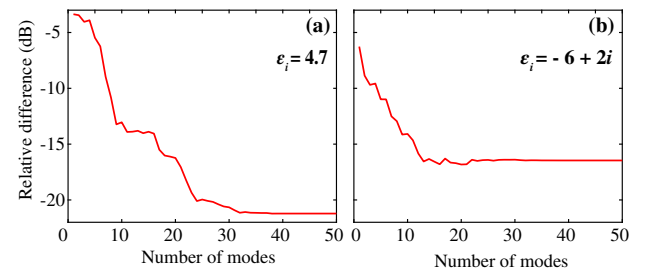


Fig. 7. L_2 norm of the relative difference between imaginary parts of field profiles of GENOME and direct COMSOL direct simulation for (a) $\epsilon_i = 4.7$ and (b) $\epsilon_i = -6 + 2i$.

To determine the convergence of GENOME over the entire simulation domain for all Green's tensor components, we use the L_2 norm metric on the relative difference between the two solutions. Since the real part of Green's tensor has unavoidable inaccuracies, we only show the norm of the imaginary part of Green's tensor. Figure 7 shows the L_2 norm as a function of the number of modes. From these plots, we observe that the agreement between the two methods improves with the number of modes. This convergence behavior provides evidence for the completeness of the eigenmode set. The observed convergence level is, however, limited to ~ -20 dB, which is similar to the convergence previously achieved with COMSOL using numerical modes [21,42]. We mention that the convergence of QNM-based numerical methods is provided in [47]. However, that was determined only at a specific position (i.e., the scatterer origin), whereas we perform an L_2 norm over the entire simulation domain. As before, we conjecture that the limited accuracy stems from the inability to find all modes with the COMSOL eigensolver. Indeed, far better convergence was obtained when the modes were calculated analytically [21,48,49]. The bulk of the computational time of this GENOME simulation is dedicated to finding the eigenmodes.

4. SUMMARY AND DISCUSSION

We have shown how to expand the electromagnetic fields and quasi-periodic Green's tensor $\bar{\bar{G}}_K(\mathbf{r}, \mathbf{r}'; \omega)$ for lossy and open periodic systems using eigenpermittivity (generalized normal) modes. These eigenpermittivity modes are defined by the Lippmann–Schwinger Eq. (A1); existing eigenfrequency solvers can be adapted to find these modes by using a simple substitution trick, as described in [21]. The GENOME implementation has numerous advantages: The modes are always discrete and orthogonal, which significantly simplifies the modal expansion representation; and the stationary nature of the modes also provides the additional benefit of a trivial normalization scheme. Most importantly, these eigenmodes form a complete basis set, which ensures that the modal expansion solution always converges toward the true scattering solution, even in the background medium.

The formalism is implemented for the example of an open waveguide array, by computing the eigenmodes using the COMSOL eigensolver and using the quasi-periodic Green's tensor of a uniform background medium, derived in Appendix C. From these components, the total field is assembled using Eq. (14). This expansion is then validated by

comparing it to the direct COMSOL scattering simulation, which showed rapid convergence of 2–3 accurate digits using only a few eigenmodes. However, the eigenmode search entails a lengthy simulation, which may limit the method's practical utility. Thus, future work should be devoted to devising a more efficient approach to compute the modes. This could be based on reduced Brillouin zone expansion [50] or on perturbative (e.g., “re-expansion”) techniques [18,48,49,51–53]. Once such an approach is implemented, it would become practical to compute other types of Green's tensors of interest. In particular, when computing the single source Green's tensor, $\bar{\bar{G}}(\mathbf{r}, \mathbf{r}'; \omega)$ would be of great importance for the study of many quantum nano-optic effects. However, it currently requires intensive computation because it must have integration over all modes across the Brillouin zone [54]. GENOME could potentially provide a rapid, efficient way to obtain this Green's tensor.

APPENDIX A: GENERALIZED NORMAL MODE EXPANSION OF GREEN'S TENSOR

We start with the eigenvalue equation that defines the eigenpermittivity modes of the unit cell, which is obtained by neglecting $E_{0,K}$ in Eq. (11):

$$s_{K,m} \mathbf{E}_{K,m}(\mathbf{r}) = -\epsilon_b k^2 \int_{\text{WSC}} \bar{\bar{G}}_{0,K}(\mathbf{r}, \mathbf{r}'; \omega) \theta^{(p=0)}(\mathbf{r}') \times \mathbf{E}_{K,m}(\mathbf{r}') d\mathbf{r}', \quad (\text{A1})$$

where $s_{K,m}$ is the m th eigenvalue,

$$s_{K,m} \equiv \frac{\epsilon_b}{\epsilon_b - \epsilon_{K,m}}, \quad (\text{A2})$$

and $\epsilon_{K,m}$ represents the eigenpermittivity of the inclusion. Choosing an eigenpermittivity contrasts with the more prevalent choice of a frequency as the eigenvalue. The most important consequence of this choice is that our modes are stationary even in the presence of absorption, even though we choose ω (hence k) and \mathbf{K} to be real. A thorough discussion of the significance and advantages of eigenpermittivities can be found in [21].

In many cases, a differential form of the eigenvalue equation is preferred, which can be directly obtained by neglecting source \mathbf{J} in Eq. (1):

$$\nabla \times (\nabla \times \mathbf{E}_m) - k^2 \epsilon(\mathbf{r}) \mathbf{E} = \frac{1}{s_{K,m}} k^2 \epsilon_b \theta^{(0)} \mathbf{E}_m. \quad (\text{A3})$$

The modes of Eq. (A3) can be calculated by modifying any existing mode search routine, such as one based on plane wave expansion or finite elements, (e.g., using COMSOL Multiphysics [21]). Once the modes are known, we can use them to expand the Lippmann–Schwinger [Eq. (11)], a procedure that we now derive.

For notational brevity, we begin by casting Eq. (11) in operator form:

$$\mathbf{E}_K = \mathbf{E}_{0,K} + u \hat{\Gamma} \hat{\theta}^{(0)} \mathbf{E}_K, \quad (\text{A4})$$

where u describes the actual permittivity of the structure ϵ_i ,

$$u \equiv \frac{\epsilon_b - \epsilon_i}{\epsilon_b}, \quad (\text{A5})$$

and where $\hat{\Gamma}$ is an integral operator incorporating the quasi-periodic Green's tensor, and $\hat{\theta}^{(0)}$ is the operator form of step function $\theta^{(0)}$; i.e.,

$$\hat{\Gamma} \hat{\theta}^{(0)} \mathbf{E}_K \equiv -\epsilon_b k^2 \int \bar{\bar{G}}_{0,K}(\mathbf{r}, \mathbf{r}'; \omega) \theta^{(0)}(\mathbf{r}') \mathbf{E}_K(\mathbf{r}') d\mathbf{r}'. \quad (\text{A6})$$

The formal solution of Eq. (A4) is

$$\mathbf{E}_K = \frac{1}{1 - u \hat{\Gamma} \hat{\theta}^{(0)}} \mathbf{E}_{0,K}. \quad (\text{A7})$$

Our solution for the unknown field \mathbf{E}_K proceeds by projecting $\mathbf{E}_{0,K}$ onto the normal modes $\mathbf{E}_{K,m}$. Specifically, we define the identity operator \hat{I} , which in bra-ket notation is

$$\hat{I} = \sum_m \hat{\theta}^{(0)} |\mathbf{E}_{K,m}\rangle \langle \mathbf{E}_{K,m}| \hat{\theta}^{(0)}. \quad (\text{A8})$$

This simple form is valid because the modes obey a biorthogonality relation [33]. In this bra-ket notation, the fields are confined to the Weigner–Seitz unit cell. By including $\hat{\theta}^{(0)}$ in \hat{I} , we expand only over the interior fields of a single unit cell. This avoids an unwieldy integral over all space, and also expands only in the region where the eigenmodes provide a complete basis. Note that this projection operator assumes that the modes are normalized within the volume of a single unit cell:

$$\langle \mathbf{E}_{K,m} | \hat{\theta}^{(0)} | \mathbf{E}_{K,m} \rangle = 1. \quad (\text{A9})$$

In that respect, we avoid normalization issues that may arise in other modal expansions since the integral is over a finite domain. We emphasize that the identity operator in Eq. (A8) sums over a set of modes that share a common \mathbf{K} , but might belong to different bands and have different levels of confinement in any open directions.

The unknown field $|\mathbf{E}_K\rangle$ is then

$$\hat{\theta}^{(0)} |\mathbf{E}_K\rangle = \sum_m \hat{\theta}^{(0)} |\mathbf{E}_{K,m}\rangle \langle \mathbf{E}_{K,m} | \frac{\hat{\theta}^{(0)}}{1 - u \hat{\Gamma} \hat{\theta}^{(0)}} | \mathbf{E}_{0,K} \rangle. \quad (\text{A10})$$

Next is the key step of GENOME. Instead of applying the operator $(1 - u \hat{\Gamma} \hat{\theta}^{(0)})^{-1}$ to $|\mathbf{E}_{0,K}\rangle$, which would result in a lengthy numerical calculation via the Born series, we exploit the freedom offered by the unified nature of the Green's tensor in Eq. (12) and Eq. (A1) to operate on the adjoint field $\langle \mathbf{E}_{K,m} |$ instead, immediately yielding a modal expansion. We invoke the adjoint form of eigenvalue Eq. (A1),

$$\langle \mathbf{E}_{K,m} | \hat{\theta}^{(0)} \hat{\Gamma} = \langle \mathbf{E}_{K,m} | s_{K,m}. \quad (\text{A11})$$

This obtains from Eq. (A10) the total interior field $\hat{\theta}^{(0)} |\mathbf{E}_K\rangle$:

$$\hat{\theta}^{(0)} |\mathbf{E}_K\rangle = \sum_m \hat{\theta}^{(0)} |\mathbf{E}_{K,m}\rangle \frac{1}{1 - u s_{K,m}} \langle \mathbf{E}_{K,m} | \hat{\theta}^{(0)} | \mathbf{E}_{0,K} \rangle, \quad (\text{A12})$$

expressed in terms of overlap integrals.

To obtain an expression also valid in the background, Eq. (A12) is inserted back into the original Lippmann–Schwinger [Eq. (A4)], this time operating $\hat{\Gamma} \hat{\theta}^{(0)}$ on $|\mathbf{E}_{K,m}\rangle$ to give

$$|E_{\mathbf{K}}\rangle = |E_{0,\mathbf{K}}\rangle + \sum_m |E_{\mathbf{K},m}\rangle \frac{us_{\mathbf{K},m}}{1 - us_{\mathbf{K},m}} \langle E_{\mathbf{K},m} | \hat{\theta}^{(0)} | E_{0,\mathbf{K}} \rangle. \quad (\text{A13})$$

Thus, with the aid of the Lippmann–Schwinger equation, we have obtained an expansion valid over all space, even though we only expanded the fields inside the structure. For convenience, Eq. (A13) can be expressed explicitly in terms of permittivities,

$$|E_{\mathbf{K}}\rangle = |E_{0,\mathbf{K}}\rangle + \sum_m |E_{\mathbf{K},m}\rangle \frac{\epsilon_i - \epsilon_b}{\epsilon_{\mathbf{K},m} - \epsilon_i} \langle E_{\mathbf{K},m} | \hat{\theta}^{(0)} | E_{0,\mathbf{K}} \rangle. \quad (\text{A14})$$

Equation (A14) expresses the total fields within the unit cell in terms of the radiation of the external sources in the uniform background, $E_{0,\mathbf{K}}$, and the modes of the structure that are excited. The explicit form of the overlap integral $\langle E_{\mathbf{K},m} | \hat{\theta}^{(0)} | E_{0,\mathbf{K}} \rangle$ is presented in Appendix B. The solution in Eq. (A14) is exact up to truncation in m , since arbitrary accuracy is possible by increasing m . The one set of eigenmodes $|E_{\mathbf{K},m}\rangle$ is applicable to all possible structure permittivities and excitations $|E_{0,\mathbf{K}}\rangle$, as the expansion requires only the evaluation of the overlap integrals, which represent a small fraction of the total simulation time. The solution [Eq. (A14)] is the most suitable form when the source $|E_{0,\mathbf{K}}\rangle$ has a known form, such as a plane wave or a beam. If, however, the source is in the near field, a second formulation is more convenient, expressed directly in terms of sources $J_{\mathbf{K}}(\mathbf{r})$ [36]. This begins by casting Eq. (12) into operator form, yielding

$$|E_{0,\mathbf{K}}\rangle = \frac{i}{\omega\epsilon_0} \hat{\Gamma} |J_{\mathbf{K}}\rangle. \quad (\text{A15})$$

After inserting into Eq. (A13), we obtain

$$|E_{\mathbf{K}}\rangle = |E_{0,\mathbf{K}}\rangle + \frac{i}{\omega\epsilon_0} \sum_m |E_{\mathbf{K},m}\rangle \frac{us_{\mathbf{K},m}}{1 - us_{\mathbf{K},m}} \langle E_{\mathbf{K},m} | \hat{\theta}^{(0)} \hat{\Gamma} |J_{\mathbf{K}}\rangle. \quad (\text{A16})$$

Again, by applying the operator $\hat{\theta}^{(0)} \hat{\Gamma}$ to $\langle E_{\mathbf{K},m} |$ via Eq. (A11) rather than to $|J_{\mathbf{K}}\rangle$, a simple solution is obtained:

$$|E_{\mathbf{K}}\rangle = |E_{0,\mathbf{K}}\rangle + \frac{i}{\omega\epsilon_0} \sum_m |E_{\mathbf{K},m}\rangle \frac{us_{\mathbf{K},m}^2}{1 - us_{\mathbf{K},m}} \langle E_{\mathbf{K},m} | J_{\mathbf{K}} \rangle. \quad (\text{A17})$$

In terms of permittivities, Eq. (A17) can be rewritten as

$$|E_{\mathbf{K}}\rangle = |E_{0,\mathbf{K}}\rangle + \frac{i}{\omega\epsilon_0} \sum_m |E_{\mathbf{K},m}\rangle \frac{\epsilon_i - \epsilon_b}{(\epsilon_{\mathbf{K},m} - \epsilon_i)(\epsilon_{\mathbf{K},m} - \epsilon_b)} \times \langle E_{\mathbf{K},m} | J_{\mathbf{K}} \rangle. \quad (\text{A18})$$

The resulting Eq. (A18) is largely similar to Eq. (A14), but the integral $\langle E_{\mathbf{K},m} | J_{\mathbf{K}} \rangle$ is now no longer restricted to the interior of the structure, and receives contributions from all locations where $J_{\mathbf{K}}(\mathbf{r})$ is nonzero. Nevertheless, Eq. (A18) remains a rigorous solution of the Lippmann–Schwinger equation and still benefits from the completeness of the eigenmodes within the interior.

Finally, the desired normal mode expansion of the quasi-periodic Green's tensor, applicable to periodic arrays of

resonators in open and lossy systems, is obtained by choosing $J_{\mathbf{K}}(\mathbf{r})$ to be a localized Dirac-delta source so that the weight factor $\langle E_{\mathbf{K},m} | J_{\mathbf{K}} \rangle$ is simply the amplitude of the adjoint mode at the source location, $E_{\mathbf{K},m}^\dagger(\mathbf{r})$. The quasi-periodic Green's tensor is then

$$\bar{\bar{G}}_{\mathbf{K}}(\mathbf{r}, \mathbf{r}'; \omega) = \bar{\bar{G}}_{0,\mathbf{K}}(\mathbf{r}, \mathbf{r}'; \omega) + \frac{1}{k^2} \sum_m \frac{\epsilon_i - \epsilon_b}{(\epsilon_{\mathbf{K},m} - \epsilon_i)(\epsilon_{\mathbf{K},m} - \epsilon_b)} \times E_{\mathbf{K},m}(\mathbf{r}) \otimes E_{\mathbf{K},m}^\dagger(\mathbf{r}'). \quad (\text{A19})$$

APPENDIX B: ADJOINT MODES

We give the explicit forms for the overlap integrals in Eq. (A14),

$$\langle E_{\mathbf{K},m} | \hat{\theta}^{(0)} | E_{0,\mathbf{K}} \rangle = \int_{\text{WSC}} \theta^{(0)}(\mathbf{r}) E_{\mathbf{K},m}^\dagger(\mathbf{r}) \cdot E_{0,\mathbf{K}}(\mathbf{r}) d\mathbf{r}, \quad (\text{B1})$$

and in Eq. (A18),

$$\langle E_{\mathbf{K},m} | J_{\mathbf{K}} \rangle = \int_{\text{WSC}} E_{\mathbf{K},m}^\dagger(\mathbf{r}) \cdot J_{\mathbf{K}}(\mathbf{r}) d\mathbf{r}. \quad (\text{B2})$$

We know that the adjoint field $E_{\mathbf{K},m}^\dagger(\mathbf{r})$ is the left eigenstate of operator $\hat{\Gamma} \hat{\theta}^{(0)}$:

$$s_{\mathbf{K},m} \langle E_{\mathbf{K},m} | = \langle E_{\mathbf{K},m} | \hat{\Gamma} \hat{\theta}^{(0)} \quad (\text{B3})$$

and $\hat{\Gamma}$ is anti-symmetric with respect to Bloch vector \mathbf{K} as

$$\bar{\bar{G}}_{0,\mathbf{K}}(\mathbf{r}, \mathbf{r}') = \bar{\bar{G}}_{0,-\mathbf{K}}(\mathbf{r}', \mathbf{r}), \quad (\text{B4})$$

which can be proven using the Eq. (8). So the adjoint field in Eqs. (B1) and (B2) takes the form of

$$E_{\mathbf{K},m}^\dagger(\mathbf{r}) = E_{-\mathbf{K},m}(\mathbf{r}). \quad (\text{B5})$$

APPENDIX C: QUASI-PERIODIC FREE SPACE GREEN'S TENSOR

Here, we determine a rapidly converging solution of the quasi-periodic free-space Green's tensor, defined by Eq. (8), for the example shown in Fig. 1. In this 2D example, the point-dipole sources are of infinitesimal extent in two dimensions and infinite in extent in the third dimension (i.e., the z direction). The source has harmonic variation of $e^{i\beta z}$ along the third dimension.

We proceed by using the relation with the quasi-periodic Green's scalar for the scalar Helmholtz equation [16],

$$\bar{\bar{G}}_{0,\mathbf{K}}(\mathbf{r}) = \left(\bar{\bar{I}} + \frac{1}{k^2} \nabla \nabla \right) G_{0,\mathbf{K}}(\mathbf{r}), \quad (\text{C1})$$

Where, without loss of generality, we assumed that the source in the central unit cell is at the coordinate origin, so \mathbf{r} itself represents the displacement vector from the source in the central unit cell. We also extend this Green's tensor expression of free space to the uniform background medium by simply absorbing the permittivity value ϵ_b into k^2 . As our 2D example has translation invariance in the third dimension, we can write

$$\nabla = \nabla_{\perp} + i\beta \hat{z},$$

where ∇_{\perp} applies only to in-plane directions. The simplest expression of the quasi-periodic Green's scalar, $G_{0,\mathbf{K}}$ is given by

$$G_{0,\mathbf{K}}(\mathbf{r}) = \sum_p G_0(\mathbf{r} - \mathbf{R}^{(p)}) e^{i\mathbf{K} \cdot \mathbf{R}^{(p)}}, \quad (\text{C2})$$

where $G_0(\mathbf{r} - \mathbf{R}^{(p)})$ represents the Green's scalar of a isolated point source at $\mathbf{R}^{(p)}$ and the appropriate expression for $G_0(\mathbf{r} - \mathbf{R}^{(p)})$ in 2D is $iH_0(\alpha|\mathbf{r} - \mathbf{R}^{(p)}|)/4$. Therefore,

$$G_{0,\mathbf{K}}(\mathbf{r}) = \frac{i}{4} \sum_p H_0(\alpha|\mathbf{r} - \mathbf{R}^{(p)}|) e^{i\mathbf{K} \cdot \mathbf{R}^{(p)}}, \quad (\text{C3})$$

where α is the in-plane propagation constant, given by $\alpha^2 + \beta^2 = k^2$.

Equation (C3) converges very slowly, so we employ Ewald's method [55], which gives the solution as a sum of two rapidly converging components; i.e.,

$$G_{0,\mathbf{K}} = G_1 + G_2. \quad (\text{C4})$$

For our 1D lattice example in Fig. 1, with lattice constant L , Bloch wavevector $\mathbf{K} = K\hat{x}$, and the displacement vector $\mathbf{r} = x\hat{x} + y\hat{y}$, we have [56]

$$G_1 = \frac{1}{4L} \sum_{p=-\infty}^{\infty} \frac{e^{iKp x}}{\gamma_p} \left[e^{\gamma_p y} \operatorname{erfc} \left(\frac{\gamma_p L}{2a} + \frac{ay}{L} \right) + e^{-\gamma_p y} \operatorname{erfc} \left(\frac{\gamma_p L}{2a} - \frac{ay}{L} \right) \right],$$

$$G_2 = \frac{1}{4\pi} \sum_{p=-\infty}^{\infty} e^{ipKL} \sum_{n=0}^{\infty} \frac{1}{n!} \left(\frac{\alpha L}{2a} \right)^{2n} E_{n+1} \left(\frac{a^2 r_p^2}{L^2} \right), \quad (\text{C5})$$

where

$$K_p = K + p \frac{2\pi}{L}, \quad \gamma_p = (K_p^2 - \alpha^2)^{\frac{1}{2}}, \quad \text{and}$$

$$r_p = \sqrt{(x - pL)^2 + y^2}.$$

Here, erfc is the error complementary function, and E_{n+1} is exponential integral function of order $n + 1$. For optimal convergence, the parameter a in Eq. (C5) is chosen to be $\sqrt{\pi}$, as suggested in [56].

Using these G_1 and G_2 expressions, we can determine the quasi-periodic Green's tensor. In explicit form, we can write the nine components of $\bar{\bar{G}}_{0,\mathbf{K}}(\mathbf{r})$ in Cartesian form as

$$\bar{\bar{G}}_{0,\mathbf{K}}(\mathbf{r}) = \frac{1}{k^2} \begin{bmatrix} k^2 + \partial_x^2 & \partial_x \partial_y & i\beta \partial_x \\ \partial_y \partial_x & k^2 + \partial_y^2 & i\beta \partial_y \\ i\beta \partial_x & i\beta \partial_y & \alpha^2 \end{bmatrix} (G^1 + G^2). \quad (\text{C6})$$

Finally, we determine the derivatives of G_1 and G_2 . For G_1 :

$$\partial_x G_1 = \frac{i}{4L} \sum_p K_p T_p,$$

$$\partial_y G_1 = \frac{1}{4L} \sum_p e^{iKp x} \left[e^{\gamma_p y} \operatorname{erfc} \left(\frac{\gamma_p L}{2a} + \frac{ay}{L} \right) - e^{-\gamma_p y} \operatorname{erfc} \left(\frac{\gamma_p L}{2a} - \frac{ay}{L} \right) \right],$$

$$\partial_x^2 G_1 = -\frac{1}{4L} \sum_p K_p^2 T_p,$$

$$\partial_y^2 G_1 = \frac{1}{4L} \sum_p \gamma_p^2 T_p - \sum_p \frac{a}{\sqrt{\pi} L} e^{iKp x} \times \exp \left(-\left(\frac{\gamma_p L}{2a} \right)^2 - \left(\frac{ay}{L} \right)^2 \right),$$

$$\partial_{xy} G_1 = \partial_{yx} G_1 = \frac{i}{4L} \sum_p K_p e^{iKp x} \left[e^{\gamma_p y} \operatorname{erfc} \left(\frac{\gamma_p L}{2a} + \frac{ay}{L} \right) - e^{-\gamma_p y} \operatorname{erfc} \left(\frac{\gamma_p L}{2a} - \frac{ay}{L} \right) \right],$$

where

$$T_p = \frac{e^{iKp x}}{\gamma_p} \left[e^{\gamma_p y} \operatorname{erfc} \left(\frac{\gamma_p L}{2a} + \frac{ay}{L} \right) + e^{-\gamma_p y} \operatorname{erfc} \left(\frac{\gamma_p L}{2a} - \frac{ay}{L} \right) \right].$$

The partial derivatives of G_2 are

$$\partial_x G_2 = -\frac{1}{4\pi} \sum_{p=-\infty}^{\infty} e^{ipKL} \sum_{n=0}^{\infty} \frac{1}{n!} \left(\frac{\alpha L}{2a} \right)^{2n} \times E_n \left(\frac{a^2 r_p^2}{L^2} \right) \frac{2a^2 (x - pL)}{L^2},$$

$$\partial_y G_2 = -\frac{1}{4\pi} \sum_{p=-\infty}^{\infty} e^{ipKL} \sum_{n=0}^{\infty} \frac{1}{n!} \left(\frac{\alpha L}{2a} \right)^{2n} E_n \left(\frac{a^2 r_p^2}{L^2} \right) \frac{2a^2 y}{L^2},$$

$$\partial_{x^2} G_2 = -\frac{1}{4\pi} \sum_{p=-\infty}^{\infty} e^{ipKL} \sum_{n=0}^{\infty} \frac{1}{n!} \left(\frac{\alpha L}{2a} \right)^{2n} \times \left[\frac{2a^2}{L^2} E_n - \frac{4a^4 (x - pL)^2}{L^4} E_{n-1} \left(\frac{a^2 r_p^2}{L^2} \right) \right],$$

$$\partial_{y^2} G_2 = -\frac{1}{4\pi} \sum_{p=-\infty}^{\infty} e^{ipKL} \sum_{n=0}^{\infty} \frac{1}{n!} \left(\frac{\alpha L}{2a} \right)^{2n} \times \left[\frac{2a^2}{L^2} E_n - \frac{4a^4 y^2}{L^4} E_{n-1} \left(\frac{a^2 r_p^2}{L^2} \right) \right],$$

$$\partial_{xy} G_2 = \partial_{yx} G_2 = \frac{1}{4\pi} \sum_{p=-\infty}^{\infty} e^{ipKL} \sum_{n=0}^{\infty} \frac{1}{n!} \left(\frac{\alpha L}{2a} \right)^{2n} \times E_{n-1} \left(\frac{a^2 r_p^2}{L^2} \right) \frac{4a^4 (x - pL)y}{L^4}.$$

Funding. KAMIN grant; Deutsche Forschungsgemeinschaft (WE 5815/5-1)

Disclosures. The authors declare no conflicts of interest.

Data availability. Data underlying the results presented in this paper are not publicly available at this time but may be obtained from the authors upon reasonable request.

REFERENCES

- P. Russell, "Photonic crystal fibers," *Science* **299**, 358–362 (2003).
- P. Russell, "Photonic crystal fiber: finding the Holy grail," *Opt. Photon. News* **18**(7), 26–31 (2007).
- L. Frandsen, A. Lavrinenko, J. Fage-Pedersen, and P. Borel, "Photonic crystal waveguides with semi-slow light and tailored dispersion properties," *Opt. Express* **14**, 9444–9450 (2006).
- P. Colman, C. Husko, S. Combré, I. Sagnes, C. Wong, and A. D. Rossi, "Temporal solitons and pulse compression in photonic crystal waveguides," *Nat. Photonics* **4**, 862–868 (2010).
- H. Gersen, T. J. Karle, R. J. P. Engelen, W. Bogaerts, J. P. Korterik, N. F. V. Hulst, T. F. Krauss, and L. K. Kuipers, "Real-space observation of ultraslow light in photonic crystal waveguides," *Phys. Rev. Lett.* **94**, 073903 (2005).
- F. Garcia-Vidal, L. Martin-Moreno, and J. Pendry, "Surfaces with holes in them: new plasmonic metamaterials," *J. Opt. A* **7**, S97–S101 (2005).
- J. D. Joannopoulos, S. G. Johnson, J. N. Winn, and R. D. Meade, *Photonic Crystals: Molding the Flow of Light*, 2nd ed. (Princeton University, 2008).
- M. Notomi, "Manipulating light with strongly modulated photonic crystals," *Rep. Prog. Phys.* **73**, 096501 (2010).
- S. Fan, M. Yanik, M. Povinelli, and S. Sandhu, "Dynamic photonic crystals," *Opt. Photon. News* **18**(3), 41 (2007).
- D. Kleppner, "Inhibited spontaneous emission," *Phys. Rev. Lett.* **47**, 233–236 (1981).
- J. B. Khurgin, "Slow light in various media: a tutorial," *Adv. Opt. Photon.* **2**, 287–318 (2010).
- J. Bravo-Abad, A. Rodriguez, P. Bermel, S. G. Johnson, J. D. Joannopoulos, and M. Soljačić, "Enhanced nonlinear optics in photonic-crystal microcavities," *Opt. Express* **15**, 16161–16176 (2007).
- M. Soljačić and J. D. Joannopoulos, "Enhancement of nonlinear effects using photonic crystals," *Nat. Mater.* **3**, 211–219 (2004).
- P. M. Johnson, A. F. Koenderink, and W. Vos, "Ultrafast switching of photonic density of states in photonic crystals," *Phys. Rev. B* **66**, 081102 (2002).
- M. Bajcsy, S. Hofferberth, V. Balic, T. Peyronel, M. Hafezi, A. Zibrov, V. Vuletic, and M. Lukin, "Efficient all-optical switching using slow light within a hollow fiber," *Phys. Rev. Lett.* **102**, 203902 (2009).
- L. Novotny and B. Hecht, *Principles of Nano-Optics* (Cambridge University, 2006).
- C. Sauvan, J. P. Hugonin, I. S. Maksymov, and P. Lalanne, "Theory of the spontaneous optical emission of nanosize photonic and plasmon resonators," *Phys. Rev. Lett.* **110**, 237401 (2013).
- E. A. Muljarov, W. Langbein, and R. Zimmermann, "Brillouin–Wigner perturbation theory in open electromagnetic systems," *Europhys. Lett.* **92**, 50010 (2010).
- W. Yan, R. Faggiani, and P. Lalanne, "Rigorous modal analysis of plasmonic nanoresonators," *Phys. Rev. B* **97**, 205422 (2018).
- P. Kristensen, J. de Lasson, and N. Gregersen, "Calculation, normalization, and perturbation of quasinormal modes in coupled cavity-waveguide systems," *Opt. Lett.* **39**, 6359–6362 (2014).
- P. Y. Chen, D. J. Bergman, and Y. Sivan, "Generalizing normal mode expansion of electromagnetic Green's tensor to lossy resonators in open systems," *Phys. Rev. Appl.* **11**, 044018 (2019).
- P. Lalanne, W. Yan, K. Vynck, C. Sauvan, and J.-P. Hugonin, "Light interaction with photonic and plasmonic resonances," *Lasers Photon. Rev.* **12**, 1700113 (2017).
- L. J. Armitage, M. B. Doost, W. Langbein, and E. A. Muljarov, "Resonant-state expansion applied to planar waveguides," *Phys. Rev. A* **89**, 053832 (2014).
- S. G. Tikhodeev, A. L. Yablonskii, E. A. Muljarov, N. A. Gippius, and T. Ishihara, "Quasiguide modes and optical properties of photonic crystal slabs," *Phys. Rev. B* **66**, 045102 (2002).
- T. Weiss, M. Mesch, M. Schäferling, H. Giessen, W. Langbein, and E. A. Muljarov, "From dark to bright: first-order perturbation theory with analytical mode normalization for plasmonic nanoantenna arrays applied to refractive index sensing," *Phys. Rev. Lett.* **116**, 237401 (2016).
- T. Weiss, M. Schäferling, H. Giessen, N. A. Gippius, S. G. Tikhodeev, W. Langbein, and E. A. Muljarov, "Analytical normalization of resonant states in photonic crystal slabs and periodic arrays of nanoantennas at oblique incidence," *Phys. Rev. B* **96**, 045129 (2017).
- S. Neale and E. A. Muljarov, "Resonant-state expansion for planar photonic crystal structures," *Phys. Rev. B* **101**, 155128 (2020).
- G. Demésy, A. Nicolet, B. Gralak, C. Geuzaine, C. Campos, and J. E. Roman, "Nonlinear eigenvalue problems with GetDP and SLEPC: eigenmode computations of frequency-dispersive photonic open structures," *Comput. Phys. Commun.* **257**, 107509 (2020).
- C. Wolff, K. Busch, and N. A. Mortensen, "Modal expansions in periodic photonic systems with material loss and dispersion," *Phys. Rev. B* **97**, 104203 (2018).
- C. Sauvan, J. P. Hugonin, R. Carminati, and P. Lalanne, "Modal representation of spatial coherence in dissipative and resonant photonic systems," *Phys. Rev. A* **89**, 043825 (2014).
- A. Raman and S. Fan, "Photonic band structure of dispersive metamaterials formulated as a Hermitian eigenvalue problem," *Phys. Rev. Lett.* **104**, 087401 (2010).
- D. J. Bergman, "Dielectric constant of a two-component granular composite: a practical scheme for calculating the pole spectrum," *Phys. Rev. B* **19**, 2359–2368 (1979).
- D. J. Bergman and D. Stroud, "Theory of resonances in the electromagnetic scattering by macroscopic bodies," *Phys. Rev. B* **22**, 3527–3539 (1980).
- M. S. Agranovich, B. Z. Katsenelenbaum, A. N. Sivov, and N. N. Voitovich, *Generalized Method of Eigenoscillations in Diffraction Theory* (Wiley-VCH, 1999).
- A. D. S. Li Ge and Y. D. Chong, "Steady-state *ab initio* laser theory: generalizations and analytic results," *Phys. Rev. A* **82**, 063824 (2010).
- A. Farhi and D. J. Bergman, "Electromagnetic eigenstates and the field of an oscillating point electric dipole in a flat-slab composite structure," *Phys. Rev. A* **93**, 063844 (2016).
- O. Schnitzer, V. Giannini, S. A. Maier, and R. V. Craster, "Surface plasmon resonances of arbitrarily shaped nanometallic structures in the small-screening length limit," *Proc. R. Soc. A* **472**, 20160258 (2016).
- C. Forestiere and G. Miano, "Material-independent modes for electromagnetic scattering," *Phys. Rev. B* **94**, 201406 (2016).
- C. Forestiere, G. Miano, G. Rubinacci, A. Tamburrino, R. Tricarico, and S. Ventre, "Volume integral formulation for the calculation of material independent modes of dielectric scatterers," *IEEE Trans. Antennas Propag.* **66**, 2505–2514 (2018).
- N. Liver, A. Nitzan, and J. Gersten, "Local fields in cavity sites of rough dielectric surfaces," *Chem. Phys. Lett.* **111**, 449–454 (1984).
- M. Pascale, G. Miano, R. Tricarico, and C. Forestiere, "Full-wave electromagnetic modes and hybridization in nanoparticle dimers," *Sci. Rep.* **9**, 14524 (2019).
- G. Rosolen, P. Y. Chen, B. Maes, and Y. Sivan, "Overcoming the bottleneck for quantum computations of complex nanophotonic structures: Purcell and Förster resonant energy transfer calculations using a rigorous mode-hybridization method," *Phys. Rev. B* **101**, 155401 (2020).
- D. J. Bergman and K.-J. Dunn, "Bulk effective dielectric constant of a composite with a periodic microgeometry," *Phys. Rev. B* **45**, 13262–13271 (1992).
- N. W. Ashcroft and N. D. Mermin, *Solid State Physics* (Brooks/Cole, 1976).
- G. Quaranta, G. Basset, O. J. F. Martin, and B. Gallinet, "Recent advances in resonant waveguide gratings," *Laser Photon. Rev.* **12**, 1800017 (2018).
- G. B. Arfken, H. J. Weber, and F. E. Harris, *Mathematical Methods for Physicists*, 7th ed. (Academic, 2013).
- P. Lalanne, W. Yan, A. Gras, C. Sauvan, J.-P. Hugonin, M. Besbes, G. Demésy, M. D. Truong, B. Gralak, F. Zolla, A. Nicolet, F. Binkowski, L.

- Zschiedrich, S. Burger, J. Zimmerling, R. Remis, P. Urbach, H. T. Liu, and T. Weiss, "Quasinormal mode solvers for resonators with dispersive materials," *J. Opt. Soc. Am. A* **36**, 686–704 (2019).
48. P. Y. Chen, Y. Sivan, and E. A. Muljarov, "An efficient solver for the generalized normal modes of non-uniform open optical resonators," *J. Comput. Phys.* **422**, 109754 (2020).
49. P. Y. Chen and Y. Sivan, "Resolving Gibbs phenomenon via a discontinuous basis in a mode solver for open optical systems," *J. Comput. Phys.* **429**, 110004 (2021).
50. M. I. Hussein, "Reduced Bloch mode expansion for periodic media band structure calculations," *Proc. R. Soc. A* **465**, 2825–2848 (2009).
51. M. B. Doost, W. Langbein, and E. A. Muljarov, "Resonant state expansion applied to two dimensional open optical systems," *Phys. Rev. A* **87**, 043827 (2013).
52. M. B. Doost, W. Langbein, and E. A. Muljarov, "Resonant-state expansion applied to three-dimensional open optical systems," *Phys. Rev. A* **90**, 013834 (2014).
53. E. A. Muljarov, "Full electromagnetic Green's dyadic of spherically symmetric open optical systems and elimination of static modes from the resonant-state expansion," *Phys. Rev. A* **101**, 053854 (2020).
54. R. L. McPhedran, L. C. Botten, J. McOrist, A. A. Asatryan, C. M. de Sterke, and N. A. Nicorovici, "Density of states functions for photonic crystals," *Phys. Rev. E* **69**, 016609 (2004).
55. P. P. Ewald, "Die berechnung optischer und elektrostatischen gitterpotentiale," *Ann. Phys.* **369**, 253–268 (1921).
56. C. M. Linton, "The Green's function for the two-dimensional Helmholtz equation in periodic domains," *J. Eng. Math.* **33**, 377–402 (2019).